falls much more steeply with decreasing temperature than is experimentally observed. We conclude that there is additional weaker magnetic exchange between different pairs of molybdenum atoms, such that it is continuous parallel to the *b* axis.

Such intermediate magnetic behavior for a metal–metal bonded halide is very unusual, but not unique, as it has also been observed in salts of $Mo_2Cl_9^{3-}$,[16] and also for a number of halides of unknown structure.[17]

Metal–metal bonding normally requires expanded d orbitals arising from a low effective nuclear charge on the metal atom, which for a ligand such as chloride can be achieved as follows:[18] (a) An early transition metal is required as is illustrated by the metal–metal bonding found in $TiCl_3$, but not in $VCl_3$ or $CrCl_3$; in $HfCl_3$, $TaCl_3$, $WCl_3$, and $ReCl_3$, but not in $OsCl_3$ or $IrCl_3$; and in $NbCl_4$ with $\alpha$-$MoCl_4$ marginal, but not in $\beta$-$MoCl_4$ or $TcCl_4$. (b) A heavy transition metal is favorable as is illustrated by the metal–metal bonding in $TaCl_3$ and $NbCl_3$, but not in $VCl_3$; in $TaCl_4$ and $NbCl_4$, but not in $VCl_4$; in $ReCl_4$ but not in $TcCl_4$; and in $WCl_4$ with $\alpha$-$MoCl_4$ marginal, but not in $\beta$-$MoCl_4$. (c) Similarly a relatively low formal oxidation state is required as is illustrated by the metal–metal bonding in $WCl_2$, $WCl_3$, and $WCl_4$, but not in $WCl_5$; and in $MoCl_2$ and $MoCl_3$ with $\alpha$-$MoCl_4$ marginal, but not in $\beta$-$MoCl_4$ or $MoCl_5$. It can be seen that the behavior of $\alpha$-$MoCl_4$ is consistent with this general pattern.

**Acknowledgments.**—We are grateful for the award of a University Research Studentship to R. M.

(16) P. W. Smith, private communication.

(17) D. Brown and R. Colton, *Nature*, **198**, 1300 (1963); *J. Chem. Soc.*, 714 (1964); R. Colton and R. L. Martin, *Nature*, **205**, 239 (1965); **207**, 141 (1965); D. F. Stewart and T. A. O'Donnell, *ibid.*, **210**, 836 (1966).

(18) K. Vrieze, Thesis, London, 1964; D. L. Kepert and K. Vrieze, "Halogen Chemistry," Vol. 3, V. Gutmann, Ed., Academic Press, London, 1967, p 1; A. F. Trotman-Dickenson, J. C. Bailar, H. J. Emeléus, and R. S. Nyholm, Ed., "Comprehensive Inorganic Chemistry," Pergamon Press, Oxford, forthcoming publication.

---

CONTRIBUTION FROM THE SCIENTIFIC LABORATORY,
FORD MOTOR COMPANY, DEARBORN, MICHIGAN

# A Molecular Orbital Study of Vibronic Interactions in the $CuCl_2$ Molecule

BY L. L. LOHR, JR.[1]

*Received May 16, 1968*

Semiempirical LCAO–MO calculations of the extended Hückel type are described for the triatomic molecule $CuCl_2$. Potential curves for both ground and excited states are presented, and computed vibrational frequencies are compared with experimental values. Spin–orbit coupling is found to alter significantly the bending curves for the Renner-active $^2\Pi_g$ and $^2\Delta_g$ crystal-field states, reducing the tendency of the linear molecule to bend on excitation. Electric-dipole oscillator strengths are computed for both the Laporte-allowed charge-transfer and the vibronic crystal-field electronic transitions. All intensities are greatest when the electric vector is parallel to the bond axis. The bending mode appears to be more effective than the antisymmetric stretching mole in inducing intensity, partly because the lower frequency of the former implies a larger temperature factor in comparing the results to the measurements of DeKock and Gruen made at 1076°K. Distribution of the vibronic intensity over spin–orbit levels is found to bring in contributions proportional to differences of the *diagonal* dipole moments of the various crystal-field states of a $C_\infty$ or $C_{2v}$ deformed molecule. The energy level and intensity calculations tend to confirm the spectral assignments of DeKock and Gruen, as opposed to those of Hougen, Leroi, and James, although some difficulty remains in obtaining sufficient vibronic intensity for the $^2\Sigma_g^+ \rightarrow {}^2\Delta_g$ absorption band, unless this band overlaps the lower energy and stronger $^2\Sigma_g^+ \rightarrow {}^2\Pi_g$ band.

## Introduction

The extended Hückel type of semiempirical LCAO–MO (linear combination of atomic orbitals–molecular orbital) scheme[2] has proved useful in describing vibronic interactions in various transition metal complexes, including the tetrahedral species[3] $VCl_4$ and $CuCl_4^{2-}$ and the octahedral complex[4] $CuCl_6^{4-}$. For these interesting Jahn–Teller systems the method yielded not only potential surfaces that were semiquantitatively correct but also wave functions from which oscillator strengths were calculated for the various crystal-field (d–d) electronic transitions. As a continuation of these studies, we present here the results of applying the MO method to the triatomic molecule $CuCl_2$. Of particular interest are the effect of bending on the orbitally degenerate $^2\Pi_g$ and $^2\Delta_g$ excited electronic states and the influence of spin–orbit coupling in modifying this Renner[5] behavior. Considerable infrared[6] and electronic[7,8] spectral data are available from gas-phase measurements for this and other[9] transition metal dihalides, while an electron spin resonance (esr) study[10] has been

(1) Department of Chemistry, University of Michigan, Ann Arbor, Mich. 48104.

(2) (a) R. Hoffmann and W. N. Lipscomb, *J. Chem. Phys.*, **36**, 2179, 3489 (1962); **37**, 2872 (1962); (b) L. L. Lohr, Jr., and W. N. Lipscomb, *ibid.*, **38**, 1607 (1963), and references contained therein.

(3) L. L. Lohr, Jr., and W. N. Lipscomb, *Inorg. Chem.*, **2**, 911 (1963).

(4) L. L. Lohr, Jr., *ibid.*, **6**, 1890 (1967).

(5) See J. A. Pople and H. C. Longuet-Higgins, *Mol. Phys.*, **1**, 372 (1958), for a description of the Renner effect in $NH_2$.

(6) G. E. Leroi, T. C. James, J. T. Hougen, and W. Klemperer, *J. Chem. Phys.*, **36**, 2879 (1962).

(7) J. T. Hougen, G. E. Leroi, and T. C. James, *ibid.*, **34**, 1670 (1961).

(8) C. W. DeKock and D. M. Gruen, *ibid.*, **44**, 4387 (1966).

(9) C. W. DeKock and D. M. Gruen, *ibid.*, **46**, 1096 (1967).

(10) P. H. Kasai, E. B. Whipple, and W. Weltner, Jr., *ibid.*, **44**, 2581 (1966).

made for the related $CuF_2$ molecule trapped in solid argon at 4°K. Thus a number of comparisons of calculated and observed properties can be made. It is also hoped that our calculations will provide a stimulus for *ab initio* studies of these small but chemically interesting molecules.

An early analysis[7] of the $CuCl_2$ absorption spectrum assigned the 2.24-eV band to the $^2\Sigma_g^+ \rightarrow {}^2\Delta_g$ transition and the 1.12-eV band to the $^2\Sigma_g^+ \rightarrow {}^2\Pi_g$ transition. However, a careful measurement[8] of the oscillator strengths ($f$) gave values of $0.8 \times 10^{-1}$ and $1.8 \times 10^{-3}$ for these bands, and it was argued that while the $f$ value for the 1.12-eV band was low enough that its assignment to a parity-forbidden d–d transition was not unreasonable, the value for the higher energy band was too great for such an assignment, and hence this band was assigned to a charge-transfer transition. New crystal-field parameters were obtained, which gave calculated excitation energies of 0.47 and 1.02 eV for excitations to the $^2\Pi_g$ and $^2\Delta_g$ states, respectively, so that the lower energy band was assigned to the higher energy crystal-field state. It was not possible in that study to look at energies below 0.5 eV (4000 $cm^{-1}$) for the missing $^2\Pi_g$ state. In view of the two different spectral assignments, a calculation of absorption intensities for both the charge-transfer and the d–d bands is of importance.

## Choice of Parameters and Variation of Geometry

The two types of parameters appearing in the LCAO–MO method in addition to the molecular geometry are the Slater exponents characterizing the valence shell AO's, which affect the orbital and total energies only *via* the overlap integrals, and the diagonal elements of an effective one-electron Hamiltonian with respect to the AO's. The latter parameters are the so-called Coulomb integrals or valence state ionization potentials (VSIP's). The initial choice of Coulomb integrals, referred to as set A, consisted of the values (all in eV): Cl(3s), −24.02; Cl(3p), −15.03; Cu(4s), −7.55; Cu(4p), −3.95; and Cu(3d), −10.60. The two Cl values are the VSIP's of Hinze and Jaffé,[11] while the three Cu values are those given by Zerner and Gouterman[12] as ionization energies from average atomic configurations and used by them in LCAO–MO calculations on transition metal porphyrins. All values correspond to choices for neutral atoms, and hence orbital exponents were obtained by Slater's rules[13] for the neutral species ($Cu^0$ with configuration $3d^{10}4s^1$) and are (in eV): Cl (3s,3p), 2.03; Cu(4s,4p), 1.00; and Cu(3d), 2.617. A second set of Coulomb integrals, set B, was also used, in which both Cl values were raised by 1.20 eV relative to those in set A, while all Cu values were lowered by the same amount. Thus in set B the difference between the Cu(3d) and Cl(3p) values is reduced by 2.40 eV from its 4.43-eV value in set A. The reason for using set B was to allow a more nearly neutral distribution of charge, as a Mulliken population analysis[14] on set A wave functions indicated a Cu charge of +2.0, while the typical set B charge is +1.5.

Variation of molecular geometry was carried out by first assuming a linear structure of $D_{\infty h}$ symmetry, making a series of calculations at different Cu–Cl bond distances to minimize the ground-state total orbital energy, whose variation is assumed[15] to match closely the variation of the total electronic energy including nuclear repulsions. Finally the bending and antisymmetric stretching nuclear coordinates are considered. Of particular interest in our study is the effect of the bending coordinate on the orbitally degenerate, Renner-active $^2\Pi_g$ and $^2\Delta_g$ excited electronic states. In set A calculations, minimum energy is found for a linear structure with a Cu–Cl distance of 2.37 Å (Figure 1). While there is no experimental value, Cu–Cl distances in crystals are about 2.3 Å.[16a] However, the Zn–Cl distance is known to be about 0.25–0.30 Å less in the molecule[16a] $ZnCl_2$ than in crystals,[16c] so that the computed Cu–Cl distance of 2.37 Å is probably at least 10% too large.

Choosing $z$ as the internuclear axis, the unpaired electron is in the mostly $Cu(3z^2 - r^2)$ MO, so that the ground state is of $^2\Sigma_g^+$ symmetry, as expected from simple crystal-field arguments. At the 2.37-Å bond distance, the $^2\Pi_g$ and $^2\Delta_g$ states, which correspond to having the unpaired electron[17] in the mostly Cu($xz$ or $yz$) and mostly Cu($xy$ or $x^2 - y^2$) MO's, have energies of 0.44 and 0.53 eV, respectively, above the ground state. If a shorter distance of 2.20 Å were chosen, these energies would be 0.68 and 0.88 eV, respectively (Figure 1). Although these larger values would improve agreement with observed spectroscopic energies, we shall restrict ourselves to the calculation of properties at the computed equilibrium distance of 2.37 Å.

Since the free-ion spin–orbit coupling parameter $\zeta_{3d}$ for Cu(II) is 0.102 eV,[18] this interaction must be included in our energy level calculations. Assuming that spin–orbit matrix elements with respect to the mostly-3d MO's will equal elements with respect to the constituent 3d AO's, the $^2\Pi_g$ and $^2\Delta_g$ states have first-order splittings of $\zeta_{3d}$ and $2\zeta_{3d}$, respectively, with the $M_J = M_L + M_S = \pm 3/2$ level lying below $M_J = \pm 1/2$ for $^2\Pi_g$ and with $M_J = \pm 5/2$ lying below $M_J = \pm 3/2$ for $^2\Delta_g$. There are also off-diagonal elements of $\zeta_{3d}(3)^{1/2}/2$ connecting $^2\Sigma_g^+$ to each orbital component of $^2\Pi_g$ and $\zeta_{3d}/2$ connecting each orbital component of $^2\Pi_g$ to each

(11) J. Hinze and H. H. Jaffé, *J. Am. Chem. Soc.*, **84**, 540 (1962).
(12) M. Zerner and M. Gouterman, *Theoret. Chim. Acta*, **4**, 44 (1966).
(13) J. C. Slater, *Phys. Rev.*, **36**, 57 (1930).
(14) R. S. Mulliken, *J. Chem. Phys.*, **23**, 1833 (1955).
(15) For a discussion of this approximation, see L. C. Allen and J. D. Russell, *ibid.*, **46**, 1029 (1967); also see J. C. Slater, "Quantum Theory of Molecules and Solids," Vol. I, McGraw-Hill Book Co., Inc., New York, N. Y., 1963, p 252.
(16) (a) Some Cu–Cl distances in crystals are: 2.22 Å in $Cs_2CuCl_4$ [L. Helmholz and R. F. Kruh, *J. Am. Chem. Soc.*, **74**, 1176 (1952)]; 2.30 and 2.65 Å in $CsCuCl_3$ [A. F. Wells, *J. Chem. Soc.*, 1662 (1947)]; 2.30, 2.33, and 2.79 Å in $(NH_4)_2CuCl_4$ [R. D. Willett, *J. Chem. Phys.*, **41**, 2243 (1964)]; and 2.30 and 2.95 Å in $CuCl_2$ [A. F. Wells, *J. Chem. Soc.*, 1670 (1947)]. (b) P. A. Akishin and V. P. Spiridonov, *Kristallografiya*, **2**, 475 (1957); *Soviet Phys. Cryst.*, **2**, 472 (1957). (c) B. Brehler, *Naturwissenschaften*, **46**, 69, 106, 554 (1959).
(17) For a $D_{\infty h}$ structure with $Cl_{1,2}$ at ±2.37 Å the $\sigma_g^+$ mostly-3d MO has the following set A composition: $0.0020(s_{1,2})$, ± $0.1919(z_{1,2})$, 0.2148. ($s_{Cu}$), and $-0.9608(z_{Cu^2})$. With set B Coulomb integrals the coefficients are: $-0.0185(s_{1,2})$, $\mp 0.2903(z_{1,2})$, $0.2423(s_{Cu})$, and $-0.9112(z_{Cu^2})$. The $\pi_g(x)$ MO is characterized in set A by $\mp 0.0982(x_{1,2})$ and $0.9963(xz_{Cu})$ and in set B by $\mp 0.1874(x_{1,2})$ and $0.9757(xz_{Cu})$. The $\delta_g$ MO's are pure 3d.
(18) C. E. Moore, National Bureau of Standards Circular No. 467, Vol. II, U. S. Government Printing Office, Washington, D. C., 1952.

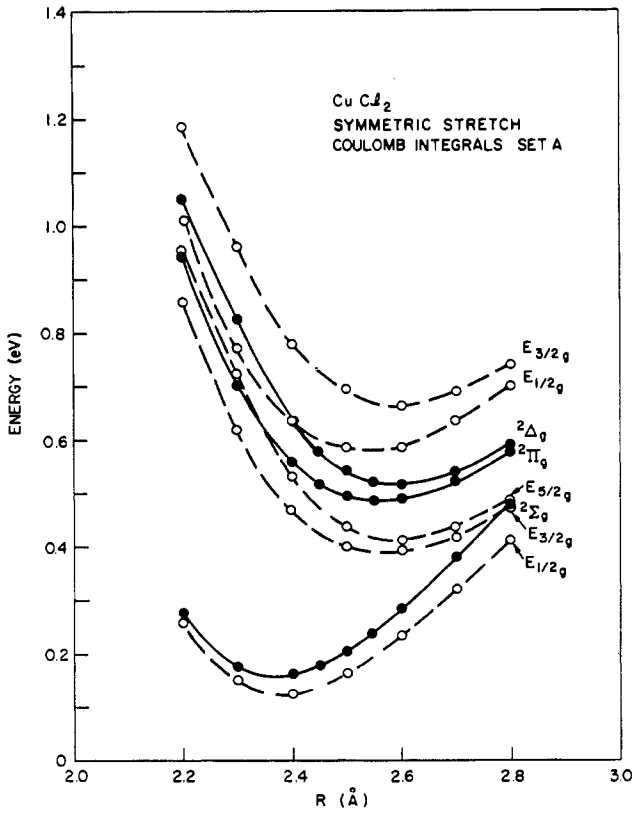


Figure 1.—Total orbital energy curves *vs.* the Cu–Cl bond length for the symmetric stretch of $CuCl_2$ with set A Coulomb integrals (see text). Solid curves give results without spin–orbit coupling and are labeled with $D_{\infty h}$ representation symbols. Dashed curves are with the spin–orbit parameter $\zeta_{3d}$ equal to 0.102 eV and are labeled by $D_{\infty h}$* symbols. The origin of energy is −373.50 eV.

orbital component of $^2\Delta_g$. While the second-order spin–orbit depression of the ground state is only 0.03 eV at 2.37 Å, the excited-state splittings are larger than the initial 0.09-eV MO energy difference, so that the five crystal-field spin–orbit levels, labeled by their $D_{\infty h}$* double-group representation symbols, increase in energy in the order: $E_{1/2g}$, $E_{3/2g}$, $E_{5/2g}$, $E_{1/2g}$, and $E_{3/2g}$, where the numerical subscript denotes the value of $|M_J|$. The four corresponding excitation energies are 0.38, 0.46, 0.55, and 0.70 eV.

The energies are obtained by diagonalizing the spin–orbit coupling within the basis of the ten states (including spin) for the unpaired electron. The LCAO–MO total orbital energies provide the diagonal matrix elements as a function of molecular geometry. This computational procedure is also convenient for obtaining electronic $g$ values, as it is easy to include matrix elements of the Zeeman interaction $\beta\mathbf{H}\cdot(\mathbf{L} + 2\mathbf{S})$, where $\beta$ is the Bohr magneton, $\mathbf{H}$ is the external magnetic field, and $\mathbf{L}$ and $\mathbf{S}$ are the electronic orbital and spin angular momentum operators.

## Potential Energy Curves and Vibrational Frequencies

The total orbital energy *vs.* geometry results with set A parameters are summarized in Figures 1–4, with solid lines indicating energies without spin–orbit coupling and dashed lines indicating energies with this interaction approximated by matrix elements with respect to pure Cu(3d) AO's. As previously mentioned, minimum energy occurs for a linear structure (Figure 1) with a bond length of 2.37 Å. The bending and antisymmetric stretching distortions were carried out with two different Cu–Cl distances: the ground-state equilibrium value (Figures 2, 3) and the $^2\Pi_g$, $^2\Delta_g$ equilibrium distance of 2.55 Å (Figure 4; the corresponding

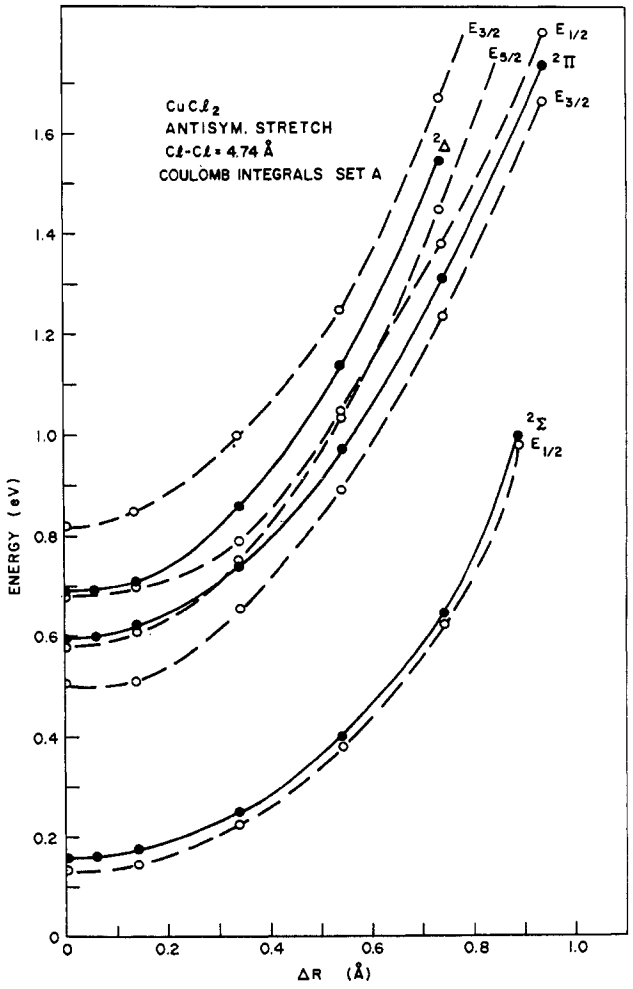


Figure 2.—Total orbital energy for the antisymmetric stretch with set A parameters. Curves are labeled by $C_{\infty v}$ (solid lines) or $C_{\infty v}$* (dashed lines) symbols. Variable is the difference in the two bond lengths whose average is 2.37 Å. See the legend for Figure 1.

figure for the antisymmetric stretch is not presented). The $M_J$ value remains a good quantum number with respect to the antisymmetric stretch, so that the $C_{\infty v}$* double-group labels in Figure 2 contain the subscript $|M_J|$. However, all electronic states of the bent molecule correspond to $E_{1/2}$ representation of the group $C_{2v}$*. Thus the inclusion of spin–orbit coupling prevents any dashed curves in Figures 3 and 4 from crossing. In particular the mixing of the $^2A_1$ ground state with the $^2B_2$ lower branch of the Renner-split $^2\Pi_g$ state significantly changes the shapes of the curves in the vicinity of bond angles of 130–140°.

It is difficult to pinpoint the expected geometry for the lower branch of the $^2\Pi_g$ state. The set A results in

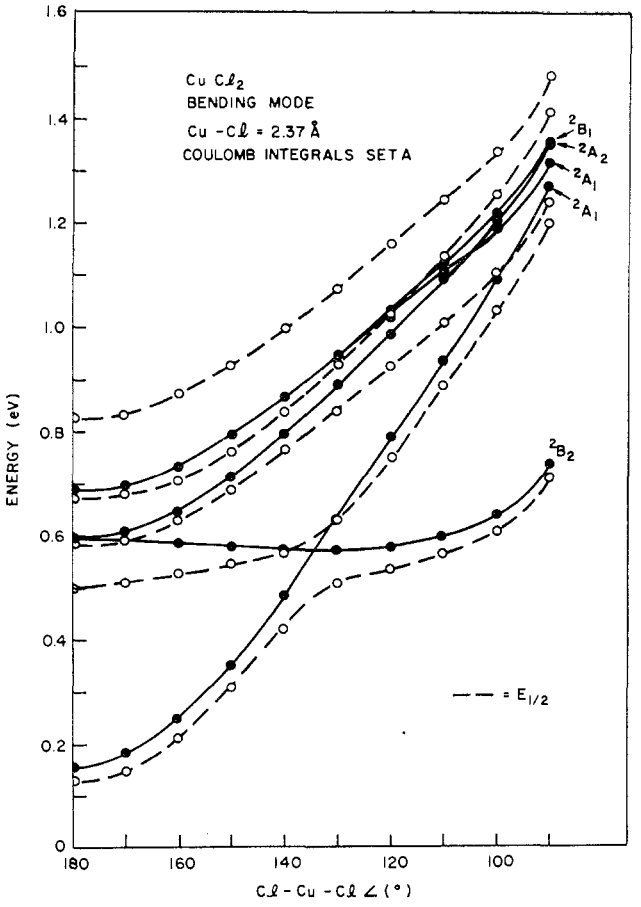


Figure 3.—Total orbital energy curves *vs.* bond angle with set A parameters and 2.37-Å bond length. Curves are labeled by $C_{2v}$ (solid lines) or $C_{2v}$* (dashed lines, all $E_{1/2}$) symbols. See the legend for Figure 1.

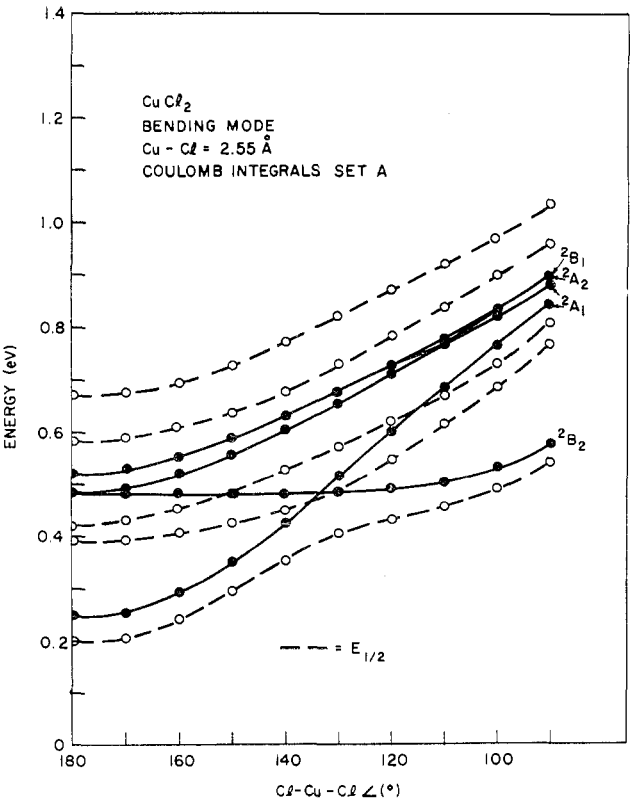


Figure 4.—Total energy curves as in Figure 3, but with 2.55-Å bond length.

Figure 4 (note that all of the $^2B_2$ points in Figure 3 suggesting a nonlinear structure lie higher than those in Figure 4) indicate a very flat potential curve. The spin–orbit interaction turns the curve upward so that the curvature is similar to that of the three levels above it. Splittings of the $^2\Delta_g$ state by bending are negligible as the unpaired electron is in one of the nonbonding $\delta$-type MO's that is pure Cu(3d) in character at 180°. The use of set B parameters (Figure 5) yields a larger splitting of $^2\Pi_g$, with a definite minimum over 0.2 eV below the $^2A_1$ curve at 110°. With spin–orbit coupling the minimum comes at 140°, and the well is much shallower, with a Renner stabilization of 0.09 eV rather than 0.29 eV. The lowest energy curve has two minima, one at 180° corresponding to the ground-state structure and the other at 110°. However in Figure 6, using the excited-state set B linear equilibrium bond length of 2.7 Å, the splitting is less pronounced as the $^2\Pi_g$ is initially stabilized by 0.17 eV in going to the larger distance. The 110° structure for the $^2B_2$ state at a Cu–Cl distance of 2.7 Å lies 0.01 eV above that at 2.37 Å, so that the Renner stabilization is only 0.11 eV. Spin–orbit coupling gives the linear structure lowest energy for this first excited $E_{1/2}$ state, and this point is 0.10 eV below the lowest point (140°) on the corresponding curve in Figure 5. Thus we conclude that spin–orbit coupling reduces the stability of a bent structure

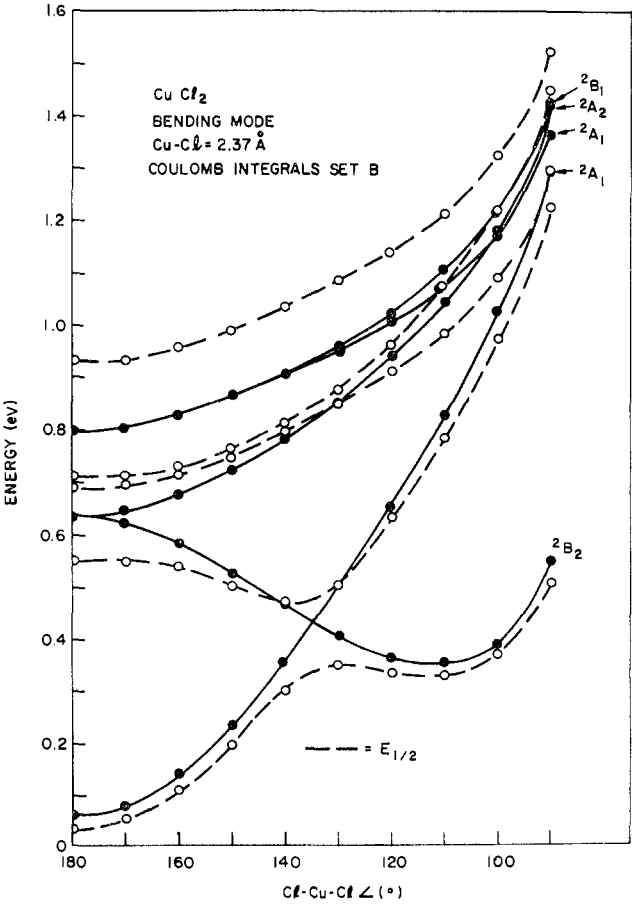


Figure 5.—Total energy curves as in Figure 3, but with set B parameters. The origin of energy is −365.10 eV.

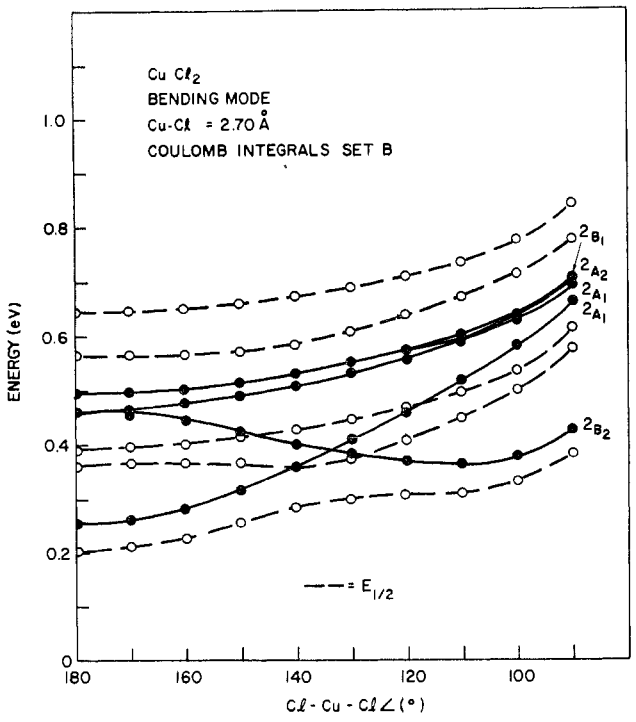


Figure 6.—Total energy curves as in Figure 5, but with 2.7-Å bond length.

for the lower branch of $^2\Pi_g$, although the bending force constant will still be smaller than that for any of the three higher energy spin–orbit levels.

The symmetric and antisymmetric stretching vibrations ($\nu_1$ and $\nu_3$) can both be approximately characterized by a bond stretching force constant $k_r$ of 0.58 mdyn/Å. With effective masses of $2m_{Cl}$ and $2m_{Cl}$ ($m_{Cu}$/MW) and the change of a bond length as the displacement variable, the computed frequences are $\nu_1$ = 167 $cm^{-1}$ and $\nu_3 = \nu_1(MW/m_{Cu})^{1/2}$ = 243 $cm^{-1}$. These values are too small, as Leroi, *et al.*, found $\nu_3$ by ir measurements[6] to be 496 $cm^{-1}$, yielding a $k_r$ value of 2.46 mdyn/Å. Their expected value of $\nu_1$ is thus 341 $cm^{-1}$, not far below the 370-$cm^{-1}$ value taken from the vibrational structure of the 1.12-eV (9000-$cm^{-1}$) electronic absorption band (DeKock and Gruen[8] similarly obtained 360 $cm^{-1}$). Note that in Figure 2 the plotted displacement variable for the antisymmetric stretch is the difference of the two Cu–Cl lengths, or twice the change of one length.

The computed bending frequency (Figure 3) is 93 $cm^{-1}$, with a force constant $k_\theta$ of 0.17 mdyn/Å based on the approximate effective mass $2m_{Cl}(m_{Cu}/MW)$, obtained from the exact mass $2m_{Cl}(1 - (2m_{Cl}\cos^2\theta/MW))$ by letting $\cos^2\theta = 1$, with the displacement variable being the product of the constant bond length in ångströms and the angle $\theta$ in radians, where the bond angle is $\pi - 2\theta$. This mode has not been observed.

When spin–orbit coupling is included (Figure 1), the $E_{1/2g}$ ground-state totally symmetric stretching frequency is slightly higher than before, 184 $cm^{-1}$. It is important to the understanding of the electronic spectrum to consider the excited-state frequencies as well. These states, in the order of increasing energy, are of symmetries $E_{3/2g}$ $E_{5/2g}$, $E_{1/2g}$, and $E_{3/2g}$, with totally symmetric stretching frequencies of 148, 168, 144, and 156 $cm^{-1}$. The corresponding increases in the equilibrium bond lengths are 0.18, 0.20, 0.15, and 0.20 Å, while the energy stabilizations (the difference between the energy at the ground-state equilibrium bond length and that at the state's own equilibrium length) are 0.09, 0.15, 0.06, and 0.13 eV, respectively. It is convenient to express these stabilizations as multiples of the corresponding stretching frequencies, giving dimensionless values of 4.8, 7.1, 3.4, and 6.6. These numbers are a measure of the Franck–Condon shift, indicating the most probable number of stretching quanta excited on absorption from the ground vibrational level of the electronic ground state. The measurements of DeKock and Gruen[8] reveal a progression of at least eight lines with separations of 360 ± 15 $cm^{-1}$, which is the assigned ground-state symmetric stretching frequency. The spectral maximum occurs at approximately the fifth quantum, which agrees well with this property of the calculated potential curves. Their measurements were made at 803°, which corresponds to a thermal energy of 748 $cm^{-1}$, or slightly over twice the vibrational frequency.

In addition to the states having the unpaired electron in one of the mostly-3d MO's, there are relatively low-energy charge-transfer (CT) states. Considering those MO's that are mostly Cl(3p) in character, the CT states will have $D_{\infty h}$ symmetries of $^2\Sigma_g^+$, $^2\Sigma_u^+$, $^2\Pi_g$, and $^2\Pi_u$. The computed energies are naturally very sensitive to the assumed difference between the Cl(3p) and Cu(3d) Coulomb integrals; with set A parameters this difference is 4.43 eV and the four excitation energies for a 2.37-Å bond length are 5.31, 4.94, 4.99, and 4.96 eV, respectively, while with set B the difference is 2.23 eV, leading to values of 3.44, 2.79, 2.88, and 2.82 eV. Even the set B values are somewhat large if the assignment of the 2.24-eV band to a CT transition is correct. One reason for the set B choice of parameters was to get a better fit of this transition, but a smaller value for the Coulomb integral difference is needed in our method to force a fit.

Dipole-allowed transitions can occur to the $^2\Sigma_u^+$ and $^2\Pi_u$ states with light polarized, respectively, parallel and perpendicular to the internuclear axis. Potential energy curves similar to those in Figures 1–4 were constructed for both of these odd-parity states, yielding for the symmetric stretch a frequency of 126 $cm^{-1}$ with set A parameters, significantly lower than the ground-state value, together with a 0.2-Å increase in the equilibrium bond length and an energy stabilization of 0.15 eV. Any computed difference between the $^2\Sigma_u^+$ and $^2\Pi_u$ states with respect to the symmetric stretch is negligible. The dimensionless ratio of the energy stabilization to the vibrational frequency is 9.6, so that the excitation of a large number of quanta of this mode is expected in the electronic spectrum. While no structure appears to have been resolved for the 2.23-eV CT band, its half-width at half-height is approximately 2500 $cm^{-1}$, as compared to about 1500 $cm^{-1}$ for the 1.12-eV d–d transition.

The $^2\Pi_u$ CT state is only slightly split by bending, so that there is no Renner stabilization for a bent structure. Even in calculations with the 2.37-Å bond length and hence with an unfavorable initial energy for this state, the total orbital energy for both branches rises upon bending, and the splitting at 160° is only 0.001 eV (set B results). For the $^2\Pi_g$ CT state the splitting at this angle is larger, 0.3 eV, but even here there is no computed stabilization for a bent structure. Thus of the four orbitally degenerate excited states we have considered, only the $^2\Pi_g$ crystal-field (d–d) state would possibly have a bent equilibrium structure, but even this result is sensitive to the choice of Coulomb integrals and to the importance of spin–orbit coupling.

### Oscillator Strengths for d–d and CT Electronic Transitions

In order to test the quality of our wave functions, electric-dipole oscillator strengths were calculated for both the "allowed" CT bands and the "forbidden" d–d bands, the latter requiring the vibronic calculational procedure described[4] for $CuCl_6^{4-}$. For both types of transitions all matrix elements of the dipole length operator **r** with respect to the AO's were calculated correctly to an accuracy of about $\pm 10^{-5}$ Å. Thus the procedure differed from that used for $CuCl_6^{4-}$ and for "allowed" transitions in $CuCl_4^{2-}$, where two-center dipole length matrix elements were approximated as the overlap integral of the two AO's times a vector directed to the midpoint of the two centers. This approximation is exact for matrix elements between equivalent nonorthogonal AO's, such as $\langle Cl_A(3p_z)|z_A|Cl_B(3p_z)\rangle$, where $z$ is the direction of the internuclear axis and the subscripts A and B denote different centers. The approximation is good for matrix elements of $z$ between nonorthogonal Cu(3d) and Cl(3s, 3p) AO's. For example, exact and approximate values for the integral $\langle Cu(3z^2 - r^2)|z_A|Cl_A(3p_z)\rangle$ are 0.09669 and 0.10132 Å, respectively, at a distance of 2.37 Å and with the AO exponents previously listed. As a result of their larger radial extent, similar approximate integrals involving Cu(4s, 4p) are too large or too small by as much as a factor of 2. Furthermore the approximation incorrectly gives a zero value to all two-center moments between orthogonal AO's, and as these moments are polarized perpendicular to the corresponding internuclear axis, an overestimation of polarizations in dipole matrix elements with respect to the MO's can result. Thus the present calculations all involve exact two-center transition moments, which were obtained by a modification of the overlap integral subroutine originally written by R. M. Stevens and used in the LCAO–MO computer program.

For polarized light and oriented molecules the electric-dipole oscillator strength $f$ is given[19] by $(4\pi m\nu/\hbar)\cdot|\mathbf{r}_{ab}|^2$, where $m$ is the electron mass, $\nu$ is the frequency of the transition in $sec^{-1}$, $\hbar$ is Planck's constant divided by $2\pi$, and $\mathbf{r}_{ab}$ is the transition moment betweens tates a and b. Using computed values for the transition energies throughout, $f$ values calculated with set A parameters at a 2.37-Å bond length for the CT transitions $^2\Sigma_g^+ \rightarrow {}^2\Sigma_u^+$ and $^2\Sigma_g^+ \rightarrow {}^2\Pi_u$ are $3.44 \times 10^{-1}$ ($\Delta E = 4.94$ eV) and $4.34 \times 10^{-3}$ ($\Delta E = 4.96$ eV). These are obtained from transition moments of 0.51588 and 0.05775 Å, respectively. The transition to $^2\Sigma_u^+$ is polarized parallel to the axis, so that the $f$ value for unpolarized light and randomly oriented molecules is obtained by dividing the oriented molecule value by 3, while that for $^2\Pi_u$, polarized perpendicular to the axis, is obtained by multiplying by $^2/_3$, giving values of $1.15 \times 10^{-1}$ and $2.89 \times 10^{-3}$, respectively. With set B parameters the transition moments are somewhat larger, 0.87433 Å for $\langle {}^2\Sigma_g^+|z|{}^2\Sigma_u^+\rangle$ and 0.08202 Å for $\langle {}^2\Sigma_g^+|x|{}^2\Pi_u(x)\rangle$, but the excitation energies are less, so that the two $f$ values are $1.84 \times 10^{-1}$ ($\Delta E = 2.79$ eV) and $3.32 \times 10^{-3}$ ($\Delta E = 2.82$ eV), both for unpolarized light and randomly oriented molecules (as will be all subsequently quoted $f$ values). Thus the computed CT $f$ values are much larger for $^2\Sigma_u^+$ than for $^2\Pi_u$, are not greatly sensitive to the choice of Coulomb integrals, and are comparable (in the case of $^2\Sigma_u^+$) to the $0.8 \times 10^{-1}$ value obtained by DeKock and Gruen for the 2.24-eV absorption band (the value[7] of Hougen, *et al.*, is $1.4 \times 10^{-2}$, but this is presumably too low owing to an incorrect assumption about the concentration of gaseous $CuCl_2$ in the sample cell).

Coupling to the antisymmetric stretching vibration, which destroys the center of inversion symmetry but preserves the $M_J$ quantum number, induces electric-dipole absorption between the $^2\Sigma^+$ ground state and the $^2\Pi$ crystal-field state, with the polarization being perpendicular to the bond axis. Again with an average Cu–Cl distance of 2.37 Å, but with a displacement giving bonds of 2.40 and 2.34 Å ($\Delta R$ of Figure 2 is 0.06 Å), the induced $\langle {}^2\Sigma^+|x|{}^2\Pi(xz)\rangle$ transition moments are −0.00052 and +0.00042 Å with parameter sets A and B, respectively, giving $f$ values of $5.57 \times 10^{-8}$ (0.44 eV) and $5.04 \times 10^{-8}$ (0.58 eV). These values for absorption at 0°K are obtained using the computed bond-stretching force constants $k_r$ of 0.58 and 0.46 mdyn/Å ($\nu_3$ values are 243 and 215 $cm^{-1}$, respectively, for parameter sets A and B). It is assumed here for simplicity that the various crystal-field states have the same antisymmetric stretching frequency, which is nearly true (see Figure 2), so that simple harmonic oscillator selection rules govern the vibronic transitions. Thus the vibronic $f$ values are proportional[4,20] to the square of a vibrational dipole matrix element and hence proportional to $k_r^{-1/2}$.

In order to compare our results with the measurements of DeKock and Gruen made[8] at 1076°K, the computed vibronic $f$ values must be multiplied[20] by $\coth(h\nu/2kT)$, where $\nu$ is the antisymmetric stretching frequency. Thus for set B, with $\nu_3 = 215$ $cm^{-1}$, a factor of 7.01 is introduced, raising the $f$ value to $3.53 \times$

(19) J. S. Griffith, "The Theory of Transition Metal Ions," Cambridge University Press, New York, N. Y., 1961, pp 41–57.

(20) C. J. Ballhausen, "Introduction to Ligand Field Theory," McGraw-Hill Book Co., Inc., New York, N. Y., 1962, pp 185–191.

$10^{-7}$. If the observed 496 $cm^{-1}$ value of $\nu_3$ were used instead, the increase would be by a factor of 3.12.

Not only are these values still much smaller than the reported $f$ value of $1.8 \times 10^{-3}$ for the 1.12-eV absorption band, but the calculated vibronic intensity due to the antisymmetric stretch is only for the low-energy $^2\Sigma_g^+ \rightarrow {}^2\Pi_g$ excitation. Thus a mechanism is needed which gives substantial intensity to $^2\Sigma_g^+ \rightarrow {}^2\Delta_g$.

Not only does coupling to the bending mode satisfy the selection rules, inducing electric-dipole intensity to both orbital components of $^2\Delta_g$, but also the low vibrational frequency favors a large temperature dependence. Using the calculated ground-state $\nu_2$ value of 93 $cm^{-1}$ at a 2.37-Å Cu–Cl distance (the $\nu_2$ value is essentially the same for sets A and B, with or without spin–orbit coupling), a temperature of 1076°K introduces a factor of 16.60 in the intensity. Furthermore the degeneracy of the bending mode means a doubling of the vibronic intensity, so that the total intensity at 1076°K will be 33.2 times that computed for a single bending mode at 0°K.

Taking $z$ to be the internuclear axis of the linear molecule, bending in the $xz$ plane induces three different d–d transition moments involving the ground state. With $x$ the $C_2$ axis, these moments are matrix elements of $z$ to the $^2B_2$ component (mostly Cu($xz$)) of $^2\Pi_g$, of $x$ to the $^2A_1$ component (mostly Cu($x^2 - y^2$)) of $^2\Delta_g$, and of $y$ (out-of-plane) to the $^2B_1$ component (mostly Cu($xy$)) of $^2\Delta_g$, where the states are labeled by the $C_{2v}$ representations used in Figures 3–6. Again these moments are very sensitive to the choice of Coulomb integrals, with the out-of-plane polarized moment equalling 0.00015 and 0.00146 Å for a 170° structure at a 2.37-Å bond length with parameter sets A and B, respectively. The set B moment yields a vibronic $f$ value of $1.74 \times 10^{-8}$ for randomly oriented molecules; with the factor of 33.2 this becomes $5.78 \times 10^{-7}$.

The in-plane $z$ moment polarized perpendicular to $C_2$ or parallel to the Cl–Cl axis of the bent molecule is −0.07140 Å for an angle of 170° with set B parameters, yielding an $f$ value of $3.26 \times 10^{-5}$ for randomly oriented molecules at 0°K. Again using the factor of 33.2, this becomes $1.08 \times 10^{-3}$ at 1076°K. Similarly the set B in-plane $x$ moment is 0.00192 Å, yielding an $f$ value of $0.99 \times 10^{-6}$ at 1076°K.

Of the three vibronic transitions associated with the bending mode, only the $z$ polarized value of $1.08 \times 10^{-3}$ for 1076°K comes anywhere near the $1.8 \times 10^{-3}$ experimental value for the 1.12-eV absorption band. The other computed values, with $x$ and $y$ polarizations, are at least three orders of magnitude too small. The difficulty remains of no appreciable vibronic intensity to $^2\Delta_g$, for the $z$ moment is to one component of $^2\Pi_g$.

One explanation for the relatively large observed intensity for the 1.12-eV d–d band would simply be that the band represents the transitions to both $^2\Pi_g$ and $^2\Delta_g$. This interpretation implies a much smaller ratio of the $^2\Sigma_g^+ \rightarrow {}^2\Delta_g$ and $^2\Sigma_g^+ \rightarrow {}^2\Pi_g$ excitation energies than the 2:1 ratio for a crystal-field model[7] with adjustable parameters. Our LCAO–MO ratios are smaller: 0.53/0.44 = 1.20 for set A and 0.74/0.58 = 1.28 for set B, both for a 2.37-Å bond length.

Another possibility is that the inclusion of spin–orbit mixes $^2\Pi_g$ and $^2\Delta_g$ enough that the latter acquires a substantial fraction of the vibronic $^2\Sigma_g^+ \rightarrow {}^2\Pi_g$ intensity. In calculating the distribution of vibronic intensity over the $M_J$ levels, contributions were found from diagonal elements of $\mathbf{r}$ with respect to the wave functions without spin–orbit coupling. We have previously demonstrated the quantum mechanical propriety of including such contributions.[21] For example, the antisymmetric stretch induces $z$-polarized intensity[22] with $\Delta M_J = 0$ between $E_{1/2g}$ (mostly $^2\Sigma_g^+$) and $E_{1/2g}$ (mostly $^2\Pi_g$); the induced transition moment with the set B unperturbed energy difference of 0.58 eV and $\zeta_{3d}$ equal to 0.102 eV is 0.1854 times the difference in the diagonal dipole moments of the unperturbed states. This difference is found in our virtual orbital approximation to be 0.02340 Å for bonds of 2.40 and 2.34 Å (average of 2.37 Å), which together with the perturbed energy difference of 0.65 eV, the computed bond stretching constant of 0.46 mdyn/Å, and the temperature factor of 7.01, yields a vibronic $f$ value of $2.12 \times 10^{-5}$ for randomly oriented molecules at 1076°K. Note that this value is about 100 times greater than the $3.53 \times 10^{-7}$ value arising from the same vibration, but polarized perpendicular to the bond axis. The latter vibronic intensity will be distributed over the $M_J$ levels according to the selection rule $\Delta M_J = \pm 1$, so that the ground level will be connected to the excited $E_{1/2}$ and to both $E_{3/2}$ levels, but not to $E_{5/2}$. Note that the transition $E_{1/2} \rightarrow E_{1/2}$, in which $\Delta|M_J|$ is zero, occurs in perpendicular polarization by the connection of $\pm 1/2$ to $\mp 1/2$. However the intensities involved here are only $10^{-7}$–$10^{-8}$, too small to consider further.

Similarly the $z$-polarized vibronic intensity induced by the bending mode, which is computed to equal $1.08 \times 10^{-3}$ (0.58 eV, set B) at 1076°K, is found to be distributed over the $D_{\infty h}$ spin–orbit levels as follows: $E_{3/2g}$, $4.44 \times 10^{-4}$ (0.52 eV); $E_{1/2g}$, $6.08 \times 10^{-4}$ (0.65 eV); and $E_{3/2g}$, $4.64 \times 10^{-5}$ (0.90 eV). The $f$ value for absorption to $E_{5/2g}$ at 0.64 eV is zero. Variation of the spin–orbit mixings with bending is not considered here, although the $z$-polarized vibronic $^2\Pi_g \rightarrow {}^2\Delta_g$ moments are needed in the calculation. These are −0.01238 Å for $\langle {}^2\Pi_g(xz)|z|{}^2\Delta_g(x^2 - y^2)\rangle$ and −0.01228 Å for $\langle {}^2\Pi_g(yz)|z|{}^2\Delta_g(xy)\rangle$, where the $C_{2v}$ wave functions are denoted by their principal Cu(3d) basis functions and $z$ is again the Cl–Cl axis. No diagonal terms enter, as only $x$ diagonal moments are induced by bending in the $xz$ plane with $x$ being the $C_2$ axis. Note that the upper $E_{3/2g}$ level, which is mostly $^2\Delta_g$, has about 10% of the intensity of the lower, mostly $^2\Pi_g$, $E_{3/2}$ level.

The distribution of the $x$-polarized vibronic intensity from the bending mode over the spin–orbit levels also involves diagonal contributions with respect to the states without spin–orbit coupling, but the principal

(21) L. L. Lohr, Jr., *J. Chem. Phys.*, **45**, 1362 (1966).

(22) If, in $C_{\infty v}$, $\Psi_0 = (1 + \alpha^2)^{-1/2}[{}^2\Sigma_{1/2}^+ + \alpha^2\Pi_{1/2}]$ and $\Psi_1 = (1 + \alpha^2)^{-1/2}[{}^2\Pi_{1/2} - \alpha^2\Sigma_{1/2}^+]$, then, for $\alpha \ll 1$, $\langle\Psi_0|z|\Psi_1\rangle = \alpha[\langle {}^2\Pi_{1/2}|z|{}^2\Pi_{1/2}\rangle - \langle {}^2\Sigma_{1/2}^+|z|{}^2\Sigma_{1/2}^+\rangle]$.

intensity involving these contributions will be for the $\Delta M_J = 0$ transition to the $E_{1/2}$ level of $^2\Pi_g$. The $x$-polarized intensity previously described to one orbital component of $^2\Delta_g$ satisfies the selection rule $\Delta M_J = \pm 2$, but is quite weak.

In summary, the largest vibronic intensity found for the $^2\Sigma_g^+ \rightarrow {}^2\Delta_g$ transition involves spin–orbit borrowing from the relatively strong $z$-polarized vibronic $^2\Sigma_g^+ \rightarrow {}^2\Pi_g$ transition induced by coupling to the degenerate bending mode. The computed value is smaller than the experimental value by a factor of 50, which may reflect either inaccuracies in the wave functions or an overlapping of absorption transitions to $^2\Pi_g$ and $^2\Delta_g$. Extension of the spectral studies to energies less than 0.5 eV to look for the $^2\Pi_g$ state is highly desirable.

Finally, it is not surprising that the vibronic moments are more sensitive than the CT moments to the difference between the Cl(3P) and Cu(3d) Coulomb integrals, for this difference largely determines the energy denominators to the CT states from which the intensity is "borrowed" in the Herzberg–Teller description.[23] It should be noted, however, that our procedure[4] works directly with adiabatic wave functions, thus avoiding the necessity of expanding the wave function for the distorted molecule on the basis of both odd- and even-parity states of the $D_{\infty h}$ molecule.[24]

**Acknowledgment.**—The author wishes to thank Mr. Gary Simons for assistance with the computations.

(23) G. Herzberg and E. Teller, *Z. Physik. Chem.*, **B21**, 410 (1933); also see A. D. Liehr, *Advan. Chem. Phys.*, **5**, 241 (1963).

(24) NOTE ADDED IN PROOF.—The bending frequencies ($\nu_2$) have recently been observed for $MnCl_2$, $FeCl_2$, $CoCl_2$, and $NiCl_2$ in matrix isolation ir experiments (K. R. Thompson and K. D. Carlson, *J. Chem. Phys.*, in press). The values range from 83 to 95 $cm^{-1}$, comparable to our calculated value of 93 $cm^{-1}$ for $CuCl_2$, but definitely greater than the 49 to 51 $cm^{-1}$ values assumed for all five dichlorides in a fit of thermodynamic properties (L Brewer, G. R. Somayajulu, and E. Brackett, *Chem. Rev.*, **63**, 111 (1963)).

---

CONTRIBUTION FROM THE CHEMISTRY DEPARTMENT OF MONTANA STATE UNIVERSITY, BOZEMAN, MONTANA 59715

# The Chemical Form of Copper(II) Acetate in Acetic Acid Solutions

BY ANDREW T. A. CHENG AND REED A. HOWALD[1]

*Received April 29, 1968*

Potentiometric measurements with glass and copper electrodes in dry and wet acetic acid solutions, together with the corresponding spectrophotometric data, show that copper(II) acetate is predominantly dimeric in dry acetic acid solutions. The dissociation constant of the dimer increases as water is added, reaching $(6 \pm 3) \times 10^{-4}$ at 3 $M$ $H_2O$. The dimer has an absorption maximum at 670 m$\mu$ with a molar absorptivity of $97.5 \pm 2.5$, while the monomer absorbs around 740 m$\mu$ with $\epsilon_{740} - \epsilon_{500} = 39 \pm 3$. The equation $\log K = -5.0 + 4 \log C_{H_2O}$ fits the data within experimental error over the range from 3 to 10 $M$ $H_2O$.

Following the determination of the crystal structure of $Cu_2(CH_3COO)_4 \cdot 2H_2O$[2] showing the presence of dimeric species with a Cu–Cu distance of 2.64 Å, there has been widespread interest in the chemical form of copper (II) acetate in solution.[3-6] It is clear from data on magnetic moment,[4] freezing points,[4] and distribution between phases[5] that the copper acetate dimers persist in solutions in dioxane and chloroform. However these studies have left the chemical form of copper acetate in solvents whose coordinating ability is greater than that of dioxane but less than that of water open to question.

The most definitive previous data on acetic acid solutions give the value of $K = 10^{-4}$ for the monomer–dimer equilibrium obtained from kinetic data.[7] This value is however inconsistent with the fact that Beer's law is followed for solutions in this region of concentrations.[8] This work was undertaken to clarify this situation. When the spectrophotometric data alone were found not to be sufficiently decisive, the study was extended to include potentiometric measurements.

The glass electrode gives quite reliable readings in "basic" acetic acid solutions.[9] The voltage of a copper electrode measured against the glass electrode should be given by the equation[10]

$$E = E^\circ - (0.05916/n) \log (C_{CuAc_2} \gamma_{CuAc_2} / a_{HAc}^2)$$

Even with considerable uncertainty in the activity coefficients it should be easy to distinguish between the values of 4 and 2 for $n$, appropriate for the dimer and monomer, respectively. If the dimeric form predominates, the equation assumes the form

$$E = E^\circ - (0.05916/4) \log (C_{Cu_2Ac_4} \gamma_{Cu_2Ac_4} / a_{HAc}^4)$$

(1) Inquiries should be directed to this author at Montana State University.

(2) J. N. van Niekerk and F. R. L. Schoening, *Acta Crystallogr.*, **6**, 227 (1953).

(3) M. Kato, H. B. Jonassen, and J. C. Fanning, *Chem. Rev.*, **64**, 99 (1964).

(4) R. L. Martin and A. Whitley, *J. Chem. Soc.*, 1394 (1958).

(5) D. P. Graddon, *Nature*, **186**, 715 (1960); *J. Inorg. Nucl. Chem.*, **17**, 222 (1961).

(6) R. Tsuchida and S. Yamada, *Nature*, **178**, 1192 (1956); S. Yamada, H. Nakamura, and R. Tsuchida, *Bull. Chem. Soc. Jap.*, **31**, 303 (1958).

(7) J. K. Kochi and R. V. Subramanian, *Inorg. Chem.*, **4**, 1527 (1965).

(8) R. P. Eswein, E. S. Howald, R. A. Howald, and D. P. Keeton, *J. Inorg. Nucl. Chem.*, **29**, 437 (1967).

(9) A. T. Cheug, R. A. Howald, and D. L. Miller, *J. Phys. Chem.*, **67**, 1601 (1963).

(10) Throughout this paper the symbol Ac is used to represent acetate, $CH_3COO$, and not acetyl.